

In Memoriam Adelina Georgescu

ATTRACTORS OF THE PERIODICALLY FORCED RAYLEIGH SYSTEM*

Petre Băzăvan[†]

Abstract

The autonomous second order nonlinear ordinary differential equation (ODE) introduced in 1883 by Lord Rayleigh, is the equation which appears to be the closest to the ODE of the harmonic oscillator with dumping.

In this paper we present a numerical study of the periodic and chaotic attractors in the dynamical system associated with the generalized Rayleigh equation. Transition between periodic and quasiperiodic motion is also studied. Numerical results describe the system dynamics changes (in particular bifurcations), when the forcing frequency is varied and thus, periodic, quasiperiodic or chaotic behaviour regions are predicted.

MSC: 34K28, 37C50, 37C70, 37G15, 37M20.

keywords: Periodic and chaotic attractors, bifurcations, Poincaré map and sections, Lyapunov exponents, periodic and quasiperiodic motion.

1 Introduction

The nonautonomous second order nonlinear ODE with time dependent sinusoidal forcing term, given by Diener [1979, 1],

$$\varepsilon \ddot{x} + \frac{\dot{x}^3}{3} - \dot{x} + ax = g \sin \omega t, \quad (1)$$

*Accepted for publication on December 16, 2010.

[†]bazavan@yahoo.com Department of Informatics, University of Craiova

is a generalisation of the Rayleigh equation $\ddot{x} + \frac{\dot{x}^3}{3} - \dot{x} + x = 0$ [Diener, 1979, 1]. Here, $x : \mathbf{R} \rightarrow \mathbf{R}$, $x = x(t)$ is the unknown function and the dot over x stands for the differentiation with respect to t . The control parameters are ε , a , g (forcing amplitude) and ω (forcing frequency).

Some aspects concerning ścanardš bifurcations are analyzed in [Diener, 1979, 1] and [Diener, 1979, 2] for the periodically forced generalization of Rayleigh equation (1). From mathematical perspective the nonautonomous system of nonlinear ODEs associated with this equation is one of a class of periodically forced nonlinear oscillators, as the van der Pol (VP) and Bonhoeffer van der Pol (BVP) systems are. The behaviour of these systems was much numerically investigated in [Flaherty and Hoppensteadt, 1978], [Mettin et al., 1993] and [Barns and Grimshaw, 1997], due to their applications in electronics and physiology.

With (1), the two-dimensional non-linear non-autonomous system of ODEs

$$\begin{cases} \dot{x}_1 = x_2, \\ \dot{x}_2 = -\frac{a}{\varepsilon}x_1 + \frac{1}{\varepsilon}\left(x_2 - \frac{x_2^3}{3}\right) + \frac{g}{\varepsilon}\sin\omega t, \end{cases} \quad (2)$$

and the three-dimensional nonlinear autonomous system

$$\begin{cases} \dot{x}_1 = x_2, \\ \dot{x}_2 = -\frac{a}{\varepsilon}x_1 + \frac{1}{\varepsilon}\left(x_2 - \frac{x_2^3}{3}\right) + \frac{g}{\varepsilon}\sin x_3, \\ \dot{x}_3 = \omega \text{ mod } 2\pi, \end{cases} \quad (3)$$

are associated. A three-dimensional dynamical system with phase space $\mathbf{R}^2 \times \mathbf{S}^1$ can be associated with (3). In [Sterpu et al., 2000], for the unforced case $g = 0$, the existence of a unique limit cycle for the dynamical system associated with the system,

$$\begin{cases} \dot{x}_1 = x_2, \\ \dot{x}_2 = -\frac{a}{\varepsilon}x_1 + \frac{1}{\varepsilon}\left(x_2 - \frac{x_2^3}{3}\right), \end{cases} \quad (4)$$

for the case $a \cdot \varepsilon > 0$, is proved.

Therefore, the system (3) without periodic forcing ($g = 0$) exhibits a natural oscillation and we consider a sinusoidal forcing imposed on it ($g \neq 0$). Fixing the parameters ε , a , and g , as ω increases away from zero, the interaction between the frequencies of these two oscillations determines the resulting dynamics. Periodic as well as chaotic motion may occur.

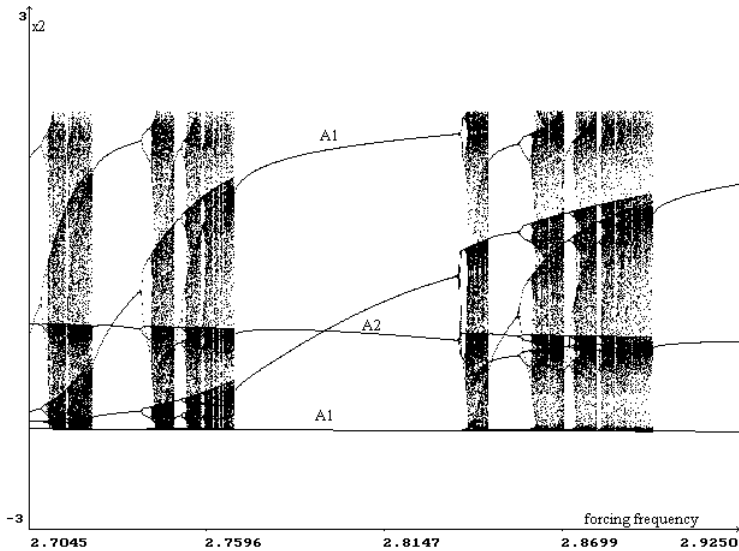


Figure 1: Bifurcation diagram for parameters $\varepsilon=0.1250$, $a=0.5$, $g=0.6666$ and $2.7045 \leq \omega \leq 2.9250$.

The lack of equilibria and the great number of parameters make the study of such a system difficult. Numerical methods often provide a useful and sometimes the only tool for study.

We intend to establish ω intervals for which specific behaviour concerning the attractors of the system (3) could be expected. By logistic reasons we investigated a region in the four-dimensional parameter space $(\varepsilon, a, g, \omega)$ given by $0 < \varepsilon \leq 1$, $0 < a \leq 1$, $0 < g \leq 1$, $2.7045 \leq \omega \leq 2.9250$ in case of Sec. 3 and $0 < \varepsilon \leq 1$, $0 < a \leq 1$, $1 < \omega \leq 3$, $0 < g \leq 2$ in case of Sec. 4.

The diagnostics used to establish structural changes of the system (3) involve representations of solutions in the phase space $\mathbf{R}^2 \times \mathbf{S}^1$, time series, Poincaré sections at intervals of forcing period $\frac{2\pi}{\omega}$, bifurcation diagrams with $\omega - x_2$ coordinates, evaluations of the eigenvalues of the linearized Poincaré map-matrix, evaluations of the Lyapunov exponents. All the numerical computations were carried out through the application of a variable step-size four order Runge-Kutta method [Băzăvan, 1999]. The 3D-representation uses a centre projection [Băzăvan, 1994].

The bifurcation diagram plotted in Fig. 1, for the case $\varepsilon = 0.1250$, $a = 0.5$, $g = 0.6666$ and ω in the interval $2.7045 \leq \omega \leq 2.9250$ shows the typical system behaviour which will be interpreted in the next sections.

The mathematical model used in our numerical study is presented in Sec. 2. The Sec. 3 is concerned with the numerical study of alternating periodic and chaotic attractors in the behaviour of the system (3). Numerical results in Sec. 4 are concerned with the proof of the existence of the quasiperiodic motion and the study of the transition from quasiperiodic to periodic motion in the system (3).

2 The mathematical model

In order to present the mathematical model used in the numerical study from Secs. 3 and 4, we shortly write (3) in the form

$$\dot{x} = f(x), \tag{5}$$

where f is defined on the $\mathbf{R}^2 \times \mathbf{S}^1$ cylinder.

We define the Poincaré map as follows. Let

$$\Sigma = \left\{ (x_1, x_2, x_3) \in \mathbf{R}^2 \times \mathbf{S}^1, \mathbf{x}_3 = \mathbf{0} \bmod \frac{2\pi}{\omega} \right\}$$

be a surface of section [Băzăvan, 2001], which is transversally crossed by the orbits of (5). The Poincaré map $P : \Sigma \rightarrow \Sigma$ is defined by

$$P(\mathbf{x}_0) = \mathbf{x}(t, \mathbf{x}_0) = \int_0^{\frac{2\pi}{\omega}} f(\mathbf{x}(t, \mathbf{x}_0)) dt, \tag{6}$$

where $x_0 \in \Sigma$ and $x(t, x_0)$ is the solution of the Cauchy problem $x(0) = x_0$ for (5). We denote by P^n the n-times iterated map.

Let $\xi(t, x_0)$ be a periodic solution of (5) with period $T = n \cdot \frac{2\pi}{\omega}$, lying on a closed orbit and consider the map P of the initial point x_0 . Then, to this closed orbit an n-periodic orbit of P corresponds. Numerically, the period T (i.e. n from the expression of T) can be determined by integrating Eq. (5) with the initial condition x_0 and sampling the orbit points $x_k = P(x_{k-1})$, $k \geq 1$ at discrete times $t_k = k \cdot \frac{2\pi}{\omega}$, until $P^k(x_0) = x_0$. Then, $n = k$ [Băzăvan, 2001].

The stability discussion of the periodic orbit $\xi(t, x_0)$ is reduced to the stability discussion of the fixed point x_0 of P^n , i.e. $P^n(x_0) = x_0$. The linear stability of the n -periodic orbit of P is determined from the linearized-map matrix DP^n of P^n . Using the Floquet theory [Reithmeier, 1991], [Glendinning, 1995] the matrix DP^n of P^n can be obtained by integrating the linearized system (5) for a small perturbation $y \in \mathbf{R}^2 \times \mathbf{S}^1$. The time history of the initial perturbation $y(0) = y_0$ is described by the linearized ODE around the periodic solution ξ .

The stability of the periodic solution $\xi(t, x_0)$ is determined by the eigenvalues of the matrix DP^n [Reithmeier, 1991], [Glendinning, 1995], [Kuznetsov, 1998]. We note that one of the eigenvalues of this matrix always equals 1 [Glendinning, 1995], and that the remained two eigenvalues, also called the Poincaré map multipliers, influence the stability. We denote these eigenvalues by λ_1 and λ_2 .

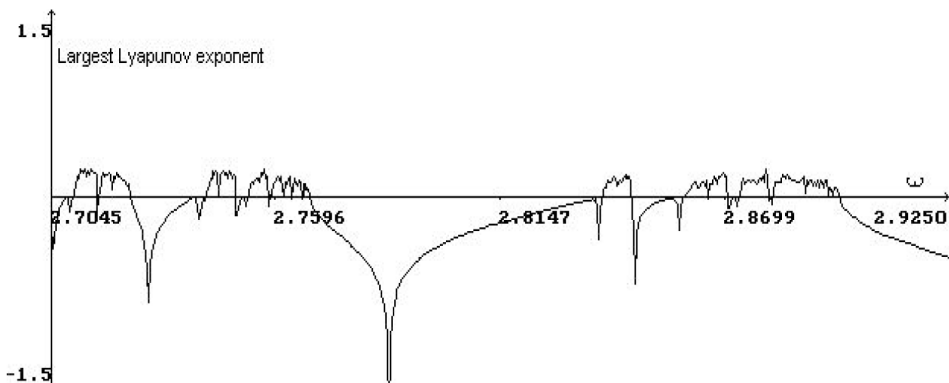


Figure 2: The largest Lyapunov exponent for (3), for parameter values $\varepsilon=0.1250$, $a=0.5$, $g=0.6666$ and $2.7045 \leq \omega \leq 2.9250$.

3 Periodic and chaotic attractors

In this section, by varying the parameter ω and keeping constant ε , a and g we study bifurcations associated with changes of stability in the periodically forced Rayleigh system (3).

The multipliers of the Poincaré map P^n , computed for $\varepsilon = 0.1250$, $a = 0.5$, $g = 0.6666$ and various ω values in the interval $2.7045 \leq \omega \leq 2.9250$, give information about the stability changes of an n -periodic orbit of (3) for which the map P is associated (see Sec. 2). Thus, the periodic orbit is stable only if $|\lambda_{1,2}| < 1$, [Reithmeier, 1991], [Glendinning, 1995], [Kuznetsov, 1998]. If, for a critical ω value, the multipliers satisfy $\lambda_1 = -1$, $-1 < \lambda_2 < 0$, [Reithmeier, 1991], [Glendinning, 1995], [Kuznetsov, 1998], the periodic orbit loses its stability through a period-doubling bifurcation. The motion becomes chaotic if, monotonically increasing ω , for sufficiently values, this process is repeated. This period doubling sequence leading to a chaotic state was reported in [Mettin, et al., 1993], [Barnes and Grimshaw, 1997] and [Sang-Yoon and Bumbi, 1998] for VP and BVP oscillators and inverted pendulum respectively. We also note that the reverse process can occur for the case of an unstable orbit. That is, when a multiplier λ of an unstable orbit increases through -1 the orbit becomes stable via period-doubling bifurcations.

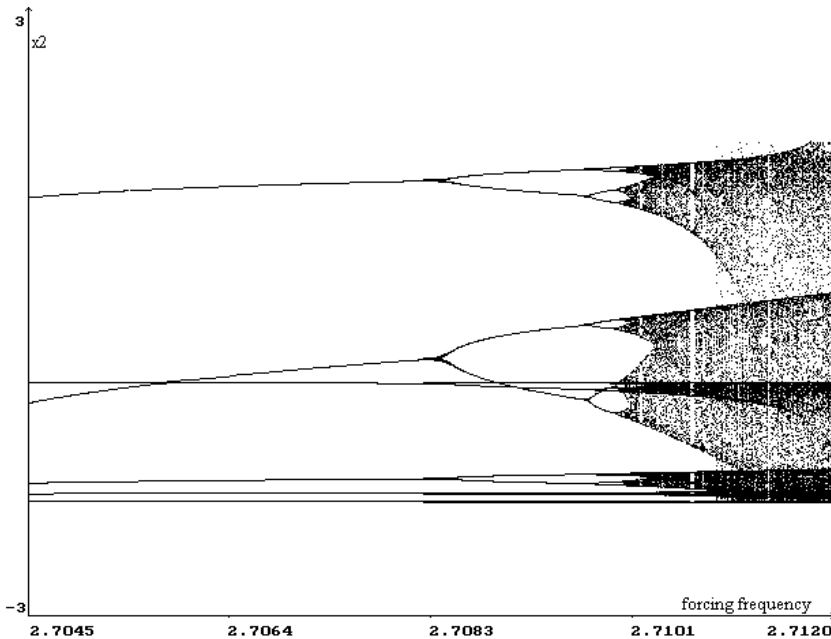


Figure 3: Bifurcation diagram for parameter values $\varepsilon=0.1250$, $a=0.5$, $g=0.6666$ and $2.7045 \leq \omega \leq 2.7120$.

As Fig. 1 shows, the system (3) exhibits the mentioned period-doubling sequences. Obvious chaotic regions interrupt periodic windows and then, chaotic attractors replace periodic attractors due to a destabilisation process through a period-doubling sequence. The reverse process, the stabilisation one, determines that periodic attractors replace chaotic attractors [Băzăvan, 2001].

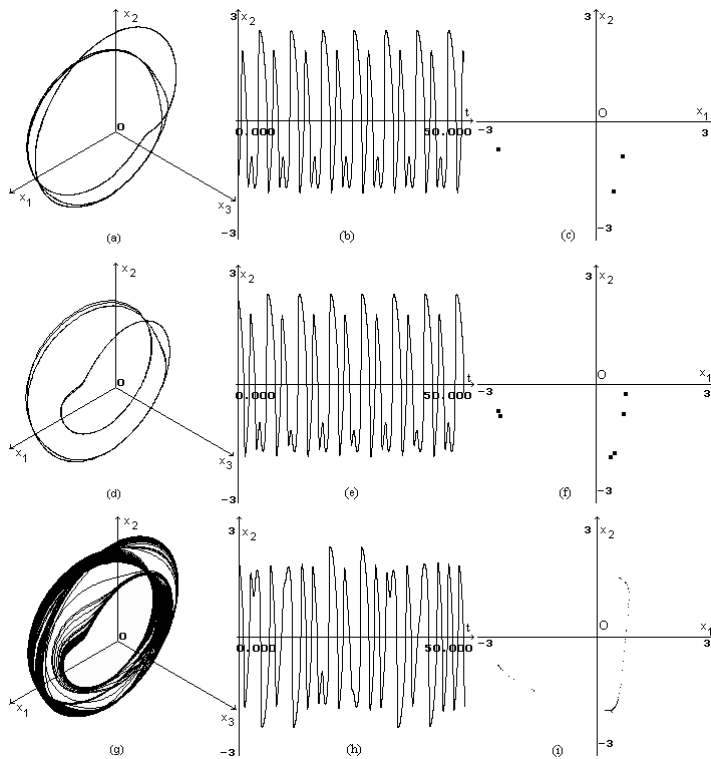


Figure 4: Closed trajectories, time series and Poincaré sections for system (3).

In order to ascertain these alternating regular and chaotic regions, the largest Lyapunov exponent measuring the convergence or divergence of neighbouring trajectories [Ott, 1993], [Barnes and Grimshaw, 1997] was plotted in Fig. 2 for the same parameter values as in Fig. 1. Negative values of this exponent correspond to periodic windows and positive values to chaotic regions.

In Fig. 3, which is a magnification of the bifurcation diagram in Fig. 1, for $2.7045 \leq \omega \leq 2.7120$, the typical route to chaotic state through a period-doubling sequence is more clearly seen. For $2.7045 \leq \omega < 2.7083$ two period-3 attractors are present.

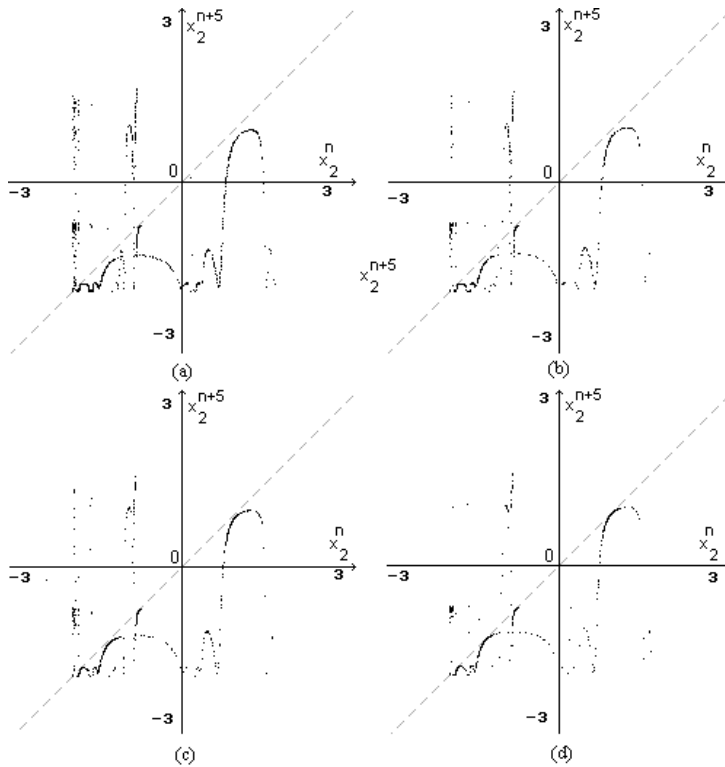


Figure 5: The points $\mathbf{X}_{n+5} = P^5(\mathbf{X}_n)$ for parameter values (a) $\omega=2.7225$, (b) $\omega=2.7230$, (c) $\omega=2.7235$, (d) $\omega=2.7240$.

The simultaneous presence of two attractors and the "jump" of the trajectories from one attractor to the other are characteristic to this system. Phase space with one of these period-3 solutions is represented on an invariant torus in Fig. 4a for $\omega = 2.7045$. For the solution in Fig. 4a, corresponding time series and Poincaré section with the three intersecting points are plotted in Figs. 4b-c. At $\omega \approx 2.7083$ the function curves split and the two solutions double their period as shows Fig. 3. The doubled periodic orbit, correspond-

ing to those from Fig. 4a, is represented in Fig. 4d for $\omega = 2.7090$. From the time series and the Poincaré section, plotted in Figs. 4e-f, the period six of the limit cycle is obvious.

The first period-doubling bifurcation at $\omega \approx 2.7083$ is followed by many subsequent period-doubling bifurcations. The length of the intervals of ω between these bifurcations decreases. Using magnifications of bifurcation diagram in Fig. 3, smaller ω step (i.e. 10^{-6}) and computing the $\lambda_{1,2}$ multipliers, for this period-doubling cascade the first five terms of the Feigenbaum progression $\frac{\omega_i - \omega_{i-1}}{\omega_{i+1} - \omega_i}$, [Kuznetsov, 1998], were estimated : 5.25, 5.18, 4.95, 4.81 and 4.72 [Băzăvan, 2001]. The convergence to the universal constant 4.6692 of this decreasing sequence is followed.

For $2.7106 < \omega < 2.7240$ the behaviour of the system is chaotic. The chaotic attractor, corresponding time series and Poincaré section are represented in Figs. 4g-i for $\omega = 2.7120$. At this ω value the largest Lyapunov exponent was computed to be 0.1812 [Băzăvan, 2001] providing the chaotic state of the system. As Fig. 1 shows, for $\omega \approx 2.7240$, the chaotic attractor is replaced by a period-5 attractor.

In order to illustrate this change from a chaotic attractor to a periodic attractor, the sequences of x_2 coordinates of the points $\mathbf{X}_{n+5} = P^5(\mathbf{X}_n)$ are plotted in Figs. 5a-d [Băzăvan, 2001]. For $\omega = 2.7225$ the diagonal $x_2^{n+5} = x_2^n$ is intersected in three separate locations. Here x_2^n represents the x_2 coordinate of the point \mathbf{X}_n . A channel between the diagonal and the return map curve is observed. As ω increases, the return map curve approaches the diagonal and at $\omega = 2.7240$ it is tangent in five distinct locations. A saddle-node bifurcation is encountered. The chaotic attractor is abruptly destroyed and replaced by a period-5 attractor. Note that, as the ω parameter increases, the density of the return points grows in the regions of the future attractor and diminishes in the other ones. This measure of the return points changes continuously with the continuous variation in the control parameter.

4 Transition between periodic and quasiperiodic motion

The dynamical system associated with (3) involves the interaction between two periodic motions, each with a different frequency. When the ratio of the frequencies is irrational the dynamical system behaves in a manner which is

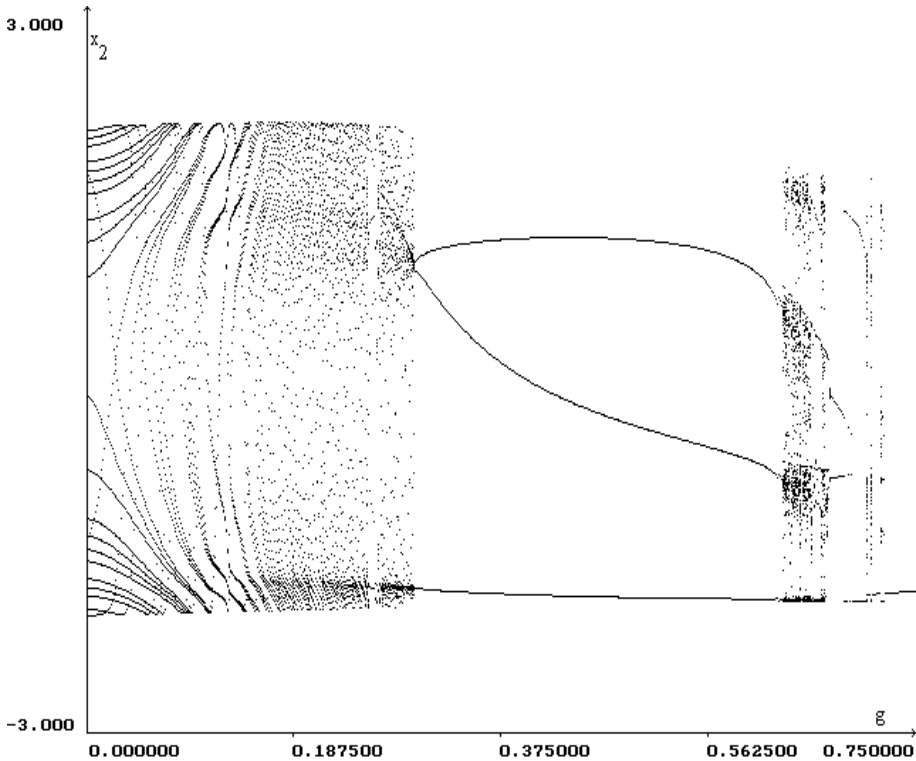


Figure 6: Bifurcation diagram for the dynamical system (3).

neither periodic or chaotic. This motion is called *quasiperiodic*. More precisely, the natural periodic motion, studied in [16] for the unforced case is modulated by a second periodic motion given by the sinusoidal term when $g > 0$. The system behaves in a manner with the motion never quite repeating any previous motion. This behaviour is generically followed by the system locking into a periodic motion, as the control parameter for the system is varied [18].

In our numerical study we investigated the region

$$\varepsilon = 0.125, \quad a = 0.5, \quad \omega = 2.84, \quad 0 < g \leq 0.75. \quad (7)$$

An overview of the numerical results which typify the system is given by the bifurcation diagram in Fig. 6.

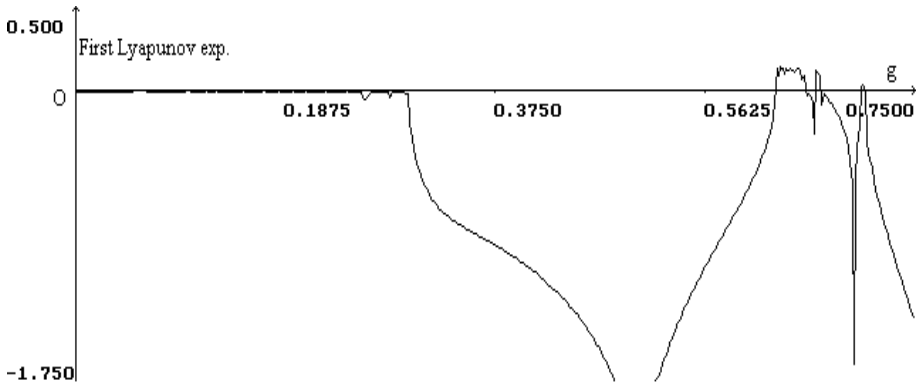


Figure 7: The first Lyapunov exponent for the dynamical system (3).

In the first part of the subinterval $0 < g < 0.3$ we observe an apparent regularity of the return points. This region which can indicate a quasiperiodic or chaotic behaviour is followed by a region with clear periodic motion. This last region is interrupted by short chaotic regions. We prove the existence of the quasiperiodic behaviour in two ways.

The first argument is the first Lyapunov exponent value. Recall that a leading Lyapunov exponent of zero verifies quasiperiodic behaviour [18].

Figure 7 is a graph of the control parameter (the forcing amplitude g) against the first Lyapunov exponent for the same parameter range as the bifurcation diagram of Fig. 6. In the interval $0 < g < 0.3$ the exponent was consistently within -0.01 of 0. This is the first numerical confirmation of the quasiperiodic behaviour.

The intersection points of the trajectories of the system (3) with the associated Poincaré section represent the second argument. At $g_1 = 0.07$ the section is represented in the Figure 8a.

The drift ring is associated with quasiperiodic motion. Integrating with a large period, the curve does not modify the shape. The fact that the points are situated on a closed curve and the constant shape related to the integration time confirm the quasiperiodic behaviour [18].

In proportion as g increases in the interval $0 < g < 0.3$ the return points remain on the same curve but the density increases markedly in some locations (Fig. 8b for $g_2 = 0.25$). At $g_3 = 0.3$ there are only three intersection points in the Poincaré section (Fig. 8c) and on the bifurcation diagram the

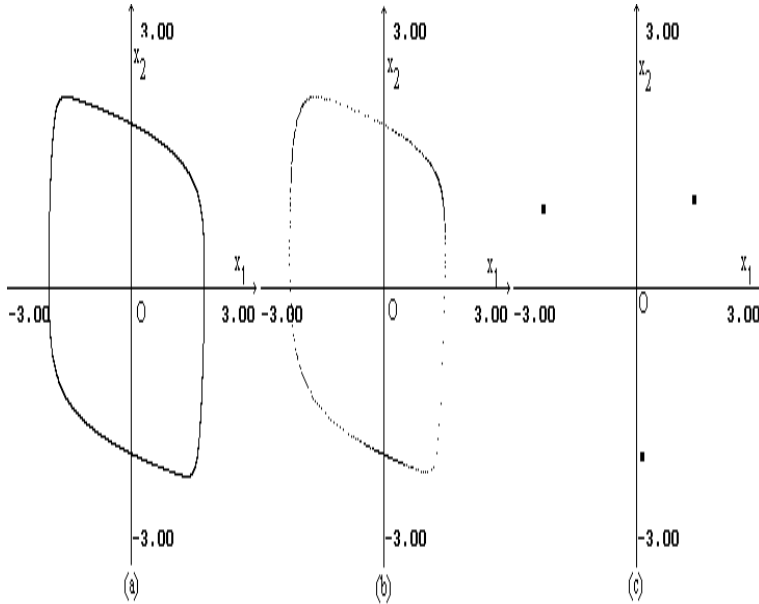


Figure 8: Poincaré sections for the dynamical system (3).

quasiperiodic region is replaced by a periodic window. The motion changes from quasiperiodic to periodic, with the emergence of a period-3 attractor. This is due to the saddle-node bifurcation of the Poincaré map P^3 ,

$$x_{n+3} = P^3(x_n), \quad x_0 \in \mathbf{R}^2 \times \mathbf{S}^1, \quad n \geq 0.$$

We numerically prove this fact. We use the projection of the graph of P^3 on the plane (y_n, y_{n+3}) , $n \geq 0$, where we denote by y the x_2 coordinate of the point $x \in \mathbf{R}^2 \times \mathbf{S}^1$.

In Figure 9a for $g_4 = 0.07$, when the motion is quasiperiodic, there are two intersection points of P^3 with the diagonal $y_n = y_{n+3}$. At the intersection the magnitude of the slope not equals 1. As g increases the curve approaches the diagonal in other locations (Fig. 9b for $g_5 = 0.28$). These locations suggest the imminent tangential intersections. At $g_6 = 0.2961$ there are three tangential intersections (Fig. 9c) and we have a saddle-node bifurcation of the map P^3 . When $g_7 = 0.3$ (Fig. 9d) the graph of the map P^3 is a single point which is situated on the diagonal. This fact confirms the existence of the period-3 attractor.

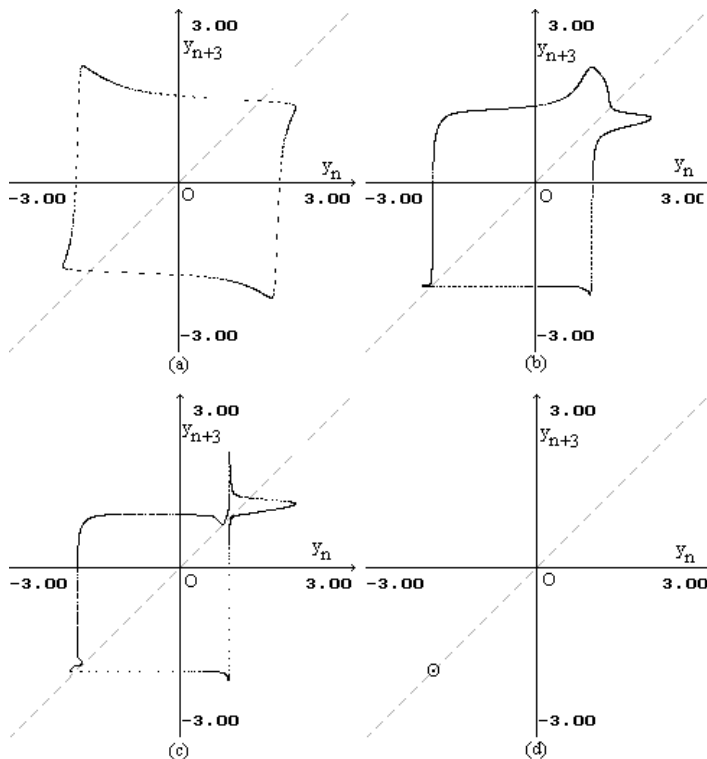


Figure 9: The Poincaré map P^3 associated with the dynamical system (3).

Conclusions

The numerical study in this paper shows that the periodically forced Rayleigh system possesses a lot of phenomena encountered in many other nonlinear systems. Some of them as period-doubling and saddle-node bifurcations, alternating periodic and chaotic attractors, alternating periodic and quasiperiodic motion, simultaneous presence of more than one periodic attractors were outlined here.

References

- [1] B. Barnes, R. Grimshaw. Numerical studies of the periodically forced Bonhoeffer van der Pol oscillator, *Int. J. Bifurcation and Chaos*, 7(12), 2653–2689, 1997.
- [2] P. Băzăvan. *Problems of Computational Geometry in "Ray-tracing"*, *Annals of University of Craiova, Romania, Math. Comp. Sci. Series XX*, 80–88, 1994.
- [3] P. Băzăvan. *The dynamical system generated by a variable step size algorithm for Runge-Kutta methods*, *Int. J. Chaos and Theory and Applications*, 4(4), 21–28, 1999.
- [4] P. Băzăvan. *Tridimensional Computation Study of Attractors for van der Pol - type Equations*, Ph.D. thesis, Institute of Mathematics of Romanian Academy, Bucharest, Romania, 2001.
- [5] M. Diener. *Nessie et les canards*, IRMA, Strasbourg, 1979.
- [6] M. Diener. *Quelques exemples de bifurcations et les canards*, *Publ. IRMA*, 37, 1979.
- [7] J.E. Flaherty, F.C. Hoppensteadt. *Frequency entrainment of a forced van der Pol oscillator*, *Studies Appl. Math*, 58, 5–15, 1978.
- [8] P. Glendinning. *Stability, Instability and Chaos*, Cambridge, New York, 1995.
- [9] E. Grebogi, E. Ott, J. Yorke. *Metamorphoses of basin boundaries in nonlinear dynamical systems*, *Phys. Rev. Lett.*, 56(10), 1011–1014, 1986.
- [10] J. Guckenheimer, P. Holmes. *Nonlinear oscillations, dynamical systems and bifurcations of vector fields*, Springer, New York, p.168, 1983.
- [11] Y. Kuznetsov. *Elements of applied bifurcation theory*, Springer Verlag, New York, 1998.
- [12] R. Mettin, U. Parlitz, W. Lauterborn *Bifurcation structure of the driven van der Pol oscillator*, *Int. J. Bifurcation and Chaos*, 3(6), 1529–1555, 1993.

- [13] E. Ott. *Chaos in dynamical systems*, Cambridge University Press, 1993.
- [14] E. Reithmeier. *Periodic Solutions of Nonlinear Dynamical Systems*, Springer Verlag, 1991.
- [15] Kim Sang-Yoon, Uh. Bumbi. Bifurcations and Transitions to Chaos in an Inverted Pendulum, Electronic paper, 1998.
- [16] M. Sterpu, P. Băzăvan. *Study on a Rayleigh equation*, Annals of University of Pitesti, Romania, Math. Comp. Sci. Series, 3, 429–434, 1999.
- [17] M. Sterpu, A. Georgescu, P. Băzăvan. *Dynamics generated by the generalized Rayleigh equation II. Periodic solutions*, Mathematical Reports, 2000, 2(52), 367–378.
- [18] G.L. Baker, J.P. Gollub. *Chaotic dynamics an introduction*, Cambridge University Press, 193-195, 1996.